Environment International 197 (2025) 109329

Contents lists available at ScienceDirect

Environment International

journal homepage: www.elsevier.com/locate/envint

Full length article

Elucidating the size distribution of *p*-Phenylenediamine-Derived quinones in atmospheric particles

Kaihui Xia [a,b,1], Meng Qin [c,1], Mingming Han [a,d], Xianming Zhang [c], Xiaoguo Wu [e], Mingyuan Liu [f], Shang Liu [g], Xinkai Wang [a], Wei Liu [a], Zhouqing Xie [a,b], Renmin Yuan [h], Qifan Liu [a,b,i,*]

[a] *Department of Environmental Science and Engineering, University of Science and Technology of China, Hefei 230026, China*
[b] *State Key Laboratory of Fire Science, University of Science and Technology of China, Hefei 230026, China*
[c] *Department of Chemistry and Biochemistry, Concordia University, 7141 Sherbrooke Street West, Montreal, QC H4B 1R6, Canada*
[d] *Department of Anesthesiology, The First Affliated Hospital of USTC, Division of Life Sciences and Medicine, University of Science and Technology of China, Hefei, Anhui 230001, China*
[e] *Anhui Provincial Engineering Laboratory of Water and Soil Pollution Control and Remediation, School of Ecology and Environment, Anhui Normal University, Wuhu, Anhui 241002, China*
[f] *Division of Ambient Air Monitoring, China National Environmental Monitoring Centre, Beijing 100012, China*
[g] *Department of Civil and Environmental Engineering, Northeastern University, Boston, MA, USA*
[h] *School of Earth and Space Sciences, University of Science and Technology of China, Hefei 230026, China*
[i] *Beijing National Laboratory for Molecular Sciences (BNLMS), Beijing 100190, China*

ARTICLE INFO

Keywords:
PPD antioxidant
PPD-quinone
Emerging contaminants
Particle size effect
Atmospheric transformation

ABSTRACT

Transformed from *p*-phenylenediamines (PPDs) antioxidant, PPD-derived quinones (PPD-Qs) have recently been recognized as emerging contaminants due to their potential negative impacts on the environment and human health. While there have been measurements of airborne PPD-Qs, the size distribution of PPD-Qs and the impact of particle size on PPD transformation chemistry remain largely unknown. Here, through the measurements of atmospheric particles in three megacities in China (Beijing, Xi'an, and Hefei), we find that PPD-Qs are widely distributed in these cities. Further analysis of the size-fractioned particles in Hefei indicates that 48 % of PPD-Qs reside in coarse particles. Given that previous studies mainly focus on the measurement of PPD-Qs in fine particles, the previously reported PPD-Q concentrations and the corresponding human exposure dosages are likely to be significantly underestimated. Furthermore, the ratio of PPD-Q to PPD concentration (PPD-Q/PPD) for particles with size range of 0.056 – 0.1 μm is up to 3 times higher than that with size range of 10 – 18 μm, highlighting the key role of particle size in determining the atmospheric oxidation reactivity of PPDs. Model simulations reveal a size-dependent pattern for the estimated concentration of particulate PPD-Qs in human body. In addition, we also demonstrate that PPD-Qs can induce the formation of cellular reactive oxygen species, suggesting that they may pose risks to human health. Overall, our results emphasize the importance of considering the particle size effect when evaluating the reaction potential and exposure risk of airborne PPD-Qs.

1. Introduction

p-Phenylenediamines (PPDs) are synthetic antioxidants widely used as additives in rubber products to resist the oxidative aging of rubber (Huntink et al., 2004; Zhao et al., 2023a). The frequently used PPDs include *N*-1,3-dimethylbutyl-*N*'-phenyl-*p*-phenylenediamine (6PPD), *N*-isopropyl-*N*'-phenyl-*p*-phenylenediamine (IPPD), *N*-phenyl-*N*'-cyclohexyl-*p*-phenylenediamine (CPPD), *N,N*'-diphenyl-*p*-phenylenediamine (DPPD), *N,N*'-bis(methylphenyl)-1,4-benzenediamine (DTPD), and *N,N*'-bis(1,4-dimethylpentyl)-*p*-phenylenediamine (77PD) (U.S. EPA, 2022). The annual production volume of PPDs vary from 100 to 200,000 tons in different countries, with 6PPD being the most dominant PPD antioxidant (Rossomme et al., 2023; Zeng et al., 2023). The massive use of PPDs in rubber products, particularly in vehicle tires, can lead to

* Corresponding author.
E-mail address: liuqifan@ustc.edu.cn (Q. Liu).
[1] These authors contributed equally.

https://doi.org/10.1016/j.envint.2025.109329
Received 12 December 2024; Received in revised form 16 January 2025; Accepted 11 February 2025
Available online 14 February 2025

their emissions into the global environment (Cao et al., 2022a; Huang et al., 2021; Johannessen et al., 2022a; Johannessen et al., 2022b; Liu et al., 2019; Wu et al., 2020). Recent evidence indicates that a transformation product of 6PPD from atmospheric ozone reaction, i.e., 6PPD-quinone (6PPD-Q), can cause acute mortality in Pacific Northwest coho salmon (Tian et al., 2021). Subsequent toxicity measurements reveal that 6PPD-Q can also induce negative impacts on other animals such as brook trout, rainbow trout, and white-spotted char (Brinkmann et al., 2022; Hiki et al., 2021; Hua and Wang, 2023b; Zhao et al., 2023b). As a result, 6PPD-Q is considered as an emerging contaminant, and has gained substantial international attention.

PPDs and 6PPD-Q have been frequently detected in various environmental matrices such as water, sediments, soil, dust, and atmospheric particles over the past three years (Cao et al., 2023; Du et al., 2022; Hiki and Yamamoto, 2022; Liang et al., 2022; Maurer et al., 2023; Seiwert et al., 2022; Song et al., 2024; Wang et al., 2022a; Wang et al., 2022b; Wang et al., 2024; Wu et al., 2024; Zhu et al., 2024; Zoroufchi Benis et al., 2023; Jiang et al., 2024; Mao et al., 2024). In the atmosphere, particle-bound PPDs (e.g., 6PPD, IPPD, CPPD) and 6PPD-Q have been measured in cities across the globe, including London, New York, Buenos Aires, Leipzig, Dresden, Sydney, and Nanjing, with the sum of all measured PPDs and 6PPD-Q ranging from 1 to 14,200 pg m^{-3} and 0.17 to 7,250 pg m^{-3}, respectively (Johannessen et al., 2022b; Wang et al., 2022b; Zhang et al., 2022b; Zoroufchi Benis et al., 2023; Kuntz et al., 2024). In addition to the well-studied 6PPD-Q, few recent studies found other PPD-Qs such as IPPD-quinone (IPPD-Q), CPPD-quinone (CPPD-Q), DPPD-quinone (DPPD-Q), DTPD-quinone (DTPD-Q), and 77PD-quinone (77PD-Q; structures shown in Table S1) were also presented in the air of Guangzhou and Hong Kong, with concentrations of up to 12,400 pg m^{-3} (Cao et al., 2022a; Wang et al., 2022b). The ubiquitous presence of PPD-Qs in the atmospheric environment has stimulated concerns over their exposure risk (Zhang et al., 2022b; Zoroufchi Benis et al., 2023). For example, it was estimated that the annual exposure dosage of 6PPD-Q for adults through inhalation could be up to 0.4 μg in Nanjing, representing a non-negligible exposure pathway (Zhang et al., 2022b).

Despite these recent advances, the understanding of atmospheric PPD-Qs and their potential exposure risk is incomplete. Previous studies on atmospheric PPD-Qs mainly focus on their measurements in particulate matter with a given size (e.g., $PM_{2.5}$) (Wang et al., 2022b; Zhang et al., 2022b), while limited consideration has been given to their particle size distribution. Note that particle size may play an important role in both PPDs transformation chemistry and PPD-Qs exposure assessment. First, in theory, the heterogeneous reactivity of organic particles toward atmospheric oxidants (e.g., ozone and OH radical) can be size-dependent, as the case of palmitic acid particle (McNeill et al., 2008). This suggests that the atmospheric transformation chemistry of particulate PPDs may also be impacted by their particle size. Second, given that the exposure level of certain particle-bound contaminants (e.g., polybrominated diphenyl ethers) is highly size-dependent (Cao et al., 2019b; Li et al., 2021), a similar case may also exist for atmospheric PPD-Qs. Both factors are essential for assessing the inhalation risk of PPD-Qs. There is currently only one report of the particle size distribution of one indoor airborne PPD-Q (6PPD-Q) in waste recycling plants (Zhang et al., 2022a). However, the chemical characteristics of 6PPD-Q (i.e., a single PPD-Q contaminant) in waste recycling plants may not reflect the characteristics of other PPD-Qs in outdoor environments. Little information is available regarding the size distribution and exposure to different particle-bound PPD-Qs in outdoor environments. Also, the potential impact of particle size on PPD transformation chemistry remains unknown.

To address this knowledge gap, here, we analyzed six PPDs and the corresponding PPD-Qs in atmospheric particle samples collected in three megacities in China (Beijing, Xi'an, and Hefei). Further analysis of the composition profiles of PPDs and PPD-Qs in size-fractioned particles in Hefei reveals a clear size-dependent distribution pattern for these contaminants, and highlights the important role of particle size in determining the transformation chemistry of atmospheric PPDs. We also evaluated the human exposure level of PPD-Qs, and measured the cellular reactive oxygen species (ROS) production potential for PPD-Qs. Together, these results can advance the understanding on the size-dependent transformation of PPDs to PPD-Qs in the atmosphere as well as their exposure risks, in support of the ongoing risk evaluation efforts for these emerging contaminants.

2. Materials and methods

2.1. Materials

The target chemicals analyzed in this study include six PPDs (6PPD, IPPD, CPPD, DPPD, DTPD, and 77PD) and their transformation products (6PPD-Q, IPPD-Q, CPPD-Q, DPPD-Q, DTPD-Q, and 77PD-Q; Table S1). Details of the reagents (solvents, surrogate standards, and internal standards) used in this study can be found in the Supporting Information (SI) Text S1.

2.2. Atmospheric particle sampling

Beijing, Xi'an and Hefei are three megacities which locate in Northern China, Western China, and Eastern China, respectively. To gain a full picture of the occurrence of atmospheric PPD-Qs in different regions in China, particle samples were collected from these cities. A total of 20 atmospheric particle samples were collected on glass fiber filters using a $PM_{2.5}$ sampler (Dandong Ruite Technology, model RT-AP4; flow rate 16.7 L min^{-1}; sampling time 24 h) from June to August 2019, in China National Environmental Monitoring Centre at Beijing (40.04°N, 116.42°E) and in Urban Sports Park at Xi'an (34.35°N, 108.94°E). To investigate the particle size distribution of atmospheric PPD-Qs, 170 size-segregated particle samples were collected using a micro-orifice uniform deposit impactor (MOUDI; MSP Corporation, model 110; flow rate 30 L min^{-1}; sampling time 24 h) from June to December 2019, in the campus of University of Science and Technology of China at Hefei (117.27°E, 31.84°N). Size ranges of the captured particles include 0.056 − 0.1, 0.1 − 0.18, 0.18 − 0.32, 0.32 − 0.56, 0.56 − 1.0, 1.0 − 1.8, 1.8 − 3.2, 3.2 − 5.6, 5.6 − 10.0, and 10.0 − 18.0 μm, covering both coarse particles (> 1.8 μm) and fine particles (≤ 1.8 μm). The meteorological conditions and ozone concentrations were recorded simultaneously. All particle samples were wrapped in aluminum foil and stored at − 20 ℃ until analyzed.

2.3. Sample pretreatment and instrumental analysis

Scraps of 1/2 particle filters were shredded and spiked with surrogate standards of 2 ng. The samples were ultrasonically extracted for 15 min with 6 mL of dichloromethane, and then the extraction procedure was repeated with 6 mL of acetonitrile. After centrifugation, the combined extracts were evaporated under nitrogen to near dryness and dissolved in 0.2 mL of methanol. The samples were filtered through a 0.22 μm PTFE filter membrane and then spiked with 2 ng of internal standard before instrumental analysis.

The analytes were analyzed using an ultra-high-performance liquid chromatograph coupled with a triple-quadrupole tandem mass spectrometer (AB Sciex 4000, MA, USA). Chromatographic separation was conducted using a C18 column (Waters XBridge BEH, 2.5 μm, 2.1 mm × 100 mm), with operation details given in the SI Text S1. Multiple reaction monitoring (MRM) was used for quantitative analysis, with instrumental parameters shown in Table S2.

2.4. Quality assurance/Quality control

No rubber-related products were used during sample pretreatment. Glass fiber filters were baked at 550 ℃ for 4 h before sampling to avoid potential contamination. One procedural blank sample was included in

every batch of 10 samples to monitor laboratory background contamination. The target compounds were not detected in procedural blank samples. Also, no contamination was found in the field blank samples, validating the feasibility of the sample collection method. The recoveries of the target compounds in particulate matter spiked samples were in the range of 77.1 − 90.5 % (Table S2). Matrix effects for these compounds were calculated by comparing the response from spiked sample extracts with that of their respective standards in pure solvents. The matrix effects were determined to be 70.5 − 91.3 %, suggesting no significant ionization suppression or enhancement. The method quantification limits (MQLs) were set to the concentration in the particle matrix that generated a signal-to-noise ratio of 10 (Table S2).

2.5. Cellular reactive oxygen species (ROS) measurement

ROS are oxygen-containing molecules that have one or more unpaired electrons, which include free radicals such as hydroxyl radical, superoxide radical, and peroxyl radicals (Bates et al., 2019). ROS assay has been widely used in investigating of the oxidative potential of atmospheric particles (Bates et al., 2019; Chowdhury et al., 2019; Grange et al., 2022). Human cerebral microvascular endothelial cells (hCMEC-D3; Shanghai Anwei Biotechnology) were exposed to four PPD-Qs (6PPD-Q, IPPD-Q, CPPD-Q, and 77PPD-Q dissolved in DMSO) at three different concentrations (0.01, 0.1, and 1.0 μM; see details for the selection of these concentrations in SI Text S2). DPPD-Q and DTPD-Q experiments were not conducted due to their limited solubility in DMSO. The cellular ROS production was determined using a ROS assay kit (Beyotime Biotech Inc.). The cells (2×10^7 cells mL^{-1}) were stained with 5 μM DCFH-DA at 37 ℃ for 20 min, and then the fluorescence intensity of DCF were quantified using a flow cytometry (BD FACSCanto). The concentration of DMSO in all exposure experiments was maintained at 0.1 % (v:v). Further details regarding the cell culture can be found in the SI.

2.6. Human exposure assessment

The estimated daily intake (EDI; pg kg_{bw}^{-1} day^{-1}) of humans to PPDs and PPD-Qs through inhalation of atmospheric particles was calculated using the following equation:

$$EDI = \frac{C \times IR \times ET \times EF \times ED}{BW \times AT} \quad (1)$$

where C is the concentration of atmospheric PPDs or PPD-Qs (pg m^{-3}). IR, ET, EF, and ED represent the inhalation rates of air (m^3 h^{-1}), exposure time (h day^{-1}), exposure frequency (days $year^{-1}$), and exposure duration (years), respectively. BW and AT are human body weight (kg) and average time during exposure (days), respectively. The parameters used for EDI calculation were selected based on the recommendations of previous studies (Table S3) (Maceira et al., 2019; Wang et al., 2023; Zhang et al., 2018).

The above EDI calculation reflects the rate for chemicals to get through the external boundary of human body, often referred to as external exposure. Exposure assessment also needs to consider internal exposures using the estimated body (blood) concentration (EBC) as an endpoint. For chemicals entering the body via inhalation of atmospheric particles, EBC is influenced by the size dependent efficiency of particles trapped in respiratory system (deposition efficiency), and the absorption, distribution, metabolism and excretion processes within the body (Fig. S1). While the processes and factors affecting chemicals' concentrations are complicated, here we use a previously developed screening-level human model to link external exposure and internal exposure (see SI Text S3) (Bennett et al., 2002; U.S. EPA, 2011; Zhang et al., 2014). The model considers the efficiency of inhaled particles loaded into lungs as well as the removal of chemicals from human body due to metabolism and urination (Arnot et al., 2014; Brown, 2014; Brown et al., 2012).

2.7. Statistical analysis

Statistical analyses of targeted chemicals were performed using SPSS 25. As determined by the Shapiro − Wilk test, due to non-normality in the distribution of the concentration data, the concentration relationship between individual analytes was assessed by Spearman's correlation analysis. The difference in fluorescence intensity between different groups was checked by the Mann − Whitney U test, with statistical significance set at $p < 0.05$ and $p < 0.01$.

3. Results and discussion

3.1. PPDs and PPD-Qs in fine particles

The occurrence of atmospheric PPDs and PPD-Qs in Beijing, Xi'an, and Hefei was reported for the first time. Among the target analytes, 4 PPDs (6PPD, IPPD, CPPD, and DPPD) and 6 PPD-Qs (6PPD-Q, IPPD-Q, CPPD-Q, DPPD-Q, DTPD-Q, and 77PD-Q) were detected in all particle samples. To compare the levels of PPDs and PPD-Qs in fine particles among different cities, the $PM_{2.5}$ data from Beijing, Xi'an, and Hefei were analyzed, as summarized in Table 1. As shown in Fig. 1A, the median concentrations of total PPDs and PPD-Qs in fine particles in Beijing (44.6 and 109 pg m^{-3}, respectively) are similar to those in Xi'an (34.6 and 98.1 pg m^{-3}, respectively; Mann − Whitney U test; $p > 0.05$), but are 2.5 − 4.9 times higher than those in Hefei (9.1 and 38.7 pg m^{-3}, respectively; $p < 0.01$). The median concentrations of total PPDs and PPD-Qs in these three cities were higher than those in Leipzig, Dresden, London, and New York (total PPDs: 1.31 − 3.89 pg m^{-3}; total PPD-Qs: 0.37 − 9.51 pg m^{-3}) (Kuntz et al., 2024; Johannessen et al., 2022b). The difference in the atmospheric abundance of PPDs and PPD-Qs in these cities can be attributed to their emission sources. Abrasion of vehicle tires has been suggested as the primary pathway for PPDs to be released into the environment (Johannessen et al., 2022a; Tian et al., 2021). Indeed, high concentration of 6PPD (2.3 mg g^{-1}) was detected in tire wear particles (Zhao et al., 2023a). The higher vehicle population in Beijing and Xi'an (relative to Hefei; 3.4 − 5.9 million in Beijing and Xi'an vs. 2.2 million in Hefei) will likely lead to higher emissions of PPDs in these two cities, resulting in higher concentrations of atmospheric PPDs and the corresponding PPD-Q transformation products.

A closer inspection of the composition profile of PPDs reveal that 6PPD is the major component, which accounts for 33.8 − 53.1 % of the total PPDs in three cities (Fig. 1B). A similar trend was observed for its transformation product 6PPD-Q, which possessed the highest proportion (33.7 − 56.0 %) among the detected PPD-Qs, and had a median concentration of up to 52.1 pg m^{-3}. This is consistent with the $PM_{2.5}$ measurement results in Guangzhou, which showed that 6PPD and 6PPD-Q comprised 57 % and > 50 % of the total PPDs and PPD-Qs, respectively (Wang et al., 2022b). This is also consistent with the measurement results in other environmental media such as roadside soil in Hong Kong and sediments in South China Sea, which indicated that 6PPD and 6PPD-Q were the dominant components among the detected PPDs and PPD-Qs (Cao et al., 2022a; Zeng et al., 2023). Regardless, the higher proportion of 6PPD and 6PPD-Q in atmospheric particles is likely related to the widespread use of 6PPD in rubber products; the production volume of 6PPD is reported to be 200,000 tons in China in 2020 (Zeng et al., 2023). In addition to 6PPD-Q, IPPD-Q and DPPD-Q were also detected in the fine particles collected from three cities, with median concentrations of up to 27.9 and 28.2 pg m^{-3}, respectively. Combined with 6PPD-Q, these PPD-Qs accounted for up to 92.2 % of the total PPD-Qs, while other PPD-Qs (CPPD-Q, DTPD-Q, and 77PD-Q) had a relative lower proportion (7.8 − 15.6 %).

Further analysis of fine particle-bound PPDs and PPD-Qs in three cities indicates that individual PPDs have positive Spearman correlations with their corresponding PPD-Qs (Fig. S2). Similar atmospheric PPDs − PPD-Qs correlations were also observed in cities such as Nanjing and Shanghai (Zhang et al., 2022b). Together, the results demonstrate

Table 1
Concentrations of PPDs and PPD-Qs in fine particles ($PM_{2.5}$) from Beijing, Xi'an, and Hefei.[a]

Compounds	Beijing (pg m^{-3})			Xi'an (pg m^{-3})			Hefei (pg m^{-3})		
	Mean	Median	Range	Mean	Median	Range	Mean	Median	Range
6PPD	15.8	16.8	11.6 – 22.3	14.8	10.7	2.9 – 53.9	4.0	4.1	2.5 – 5.5
IPPD	14.5	12.2	5.7 – 26.3	13.4	13.4	8.0 – 18.4	2.1	1.7	0.8 – 5.1
CPPD	4.2	5.2	0.9 – 5.9	2.5	2.3	1.1 – 5.7	0.7	0.6	0.3 – 1.2
DPPD	9.0	8.7	3.3 – 13.9	6.5	5.3	2.5 – 11.8	2.0	1.5	0.6 – 4.7
∑PPDs	43.6	44.6	24.7 – 102	37.2	34.6	17.8 – 71.8	9.4	9.1	4.4 – 14.8
6PPD-Q	39.4	37.2	22.0 – 59.3	62.6	52.1	32.8 – 145	21.0	21.6	7.5 – 29.0
IPPD-Q	26.6	27.9	7.4 – 18.6	26.0	20.6	16.1 – 52.1	6.9	5.7	2.2 – 19.4
CPPD-Q	6.6	6.9	4.2 – 8.0	7.4	7.7	3.2 – 14.3	1.5	1.3	0.7 – 2.9
DPPD-Q	32.0	28.2	21.6 – 61.3	16.1	13.6	9.4 – 32.8	8.0	6.9	2.2 – 10.5
DTPD-Q	6.4	6.0	3.5 – 11.2	6.1	5.4	3.2 – 12.5	1.3	1.1	0.1 – 4.5
77PD-Q	4.5	4.2	2.2 – 7.4	2.8	2.0	0.8 – 8.6	0.4	0.3	0.1 – 1.4
∑PPD-Qs	116	109	89.7 – 169	121	98.1	85.7 – 240	37.8	38.7	18.9 – 60.5

[a] The defection frequencies for PPDs and PPD-Qs are 100%. The measured concentrations of PM_{18} -bound PPDs and PPD-Qs in Hefei are shown in Table S5.

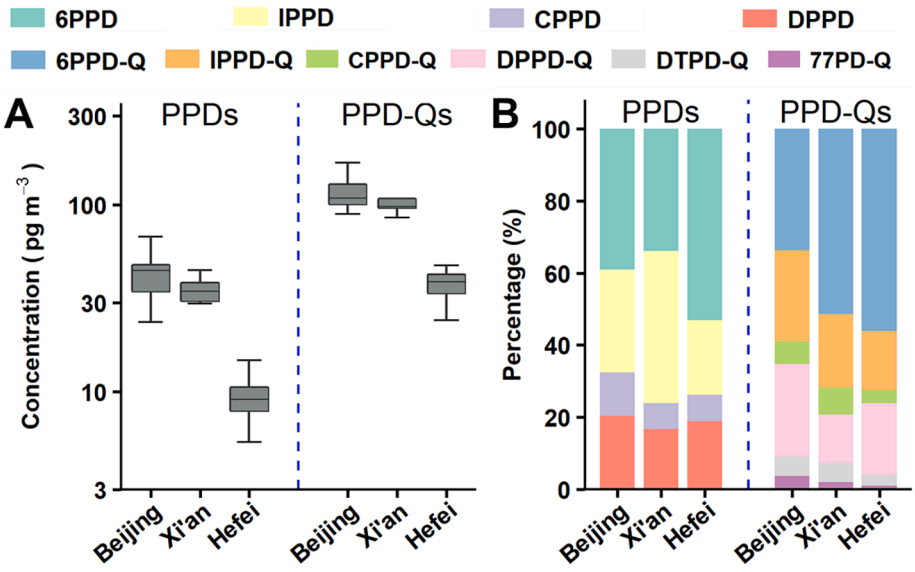

Fig. 1. Atmospheric concentrations (**A**) and composition profiles (**B**) of fine particle-bound PPDs and PPD-Qs in Beijing, Xi'an, and Hefei. The measurement results in Beijing, Xi'an and Hefei are based on $PM_{2.5}$ data.

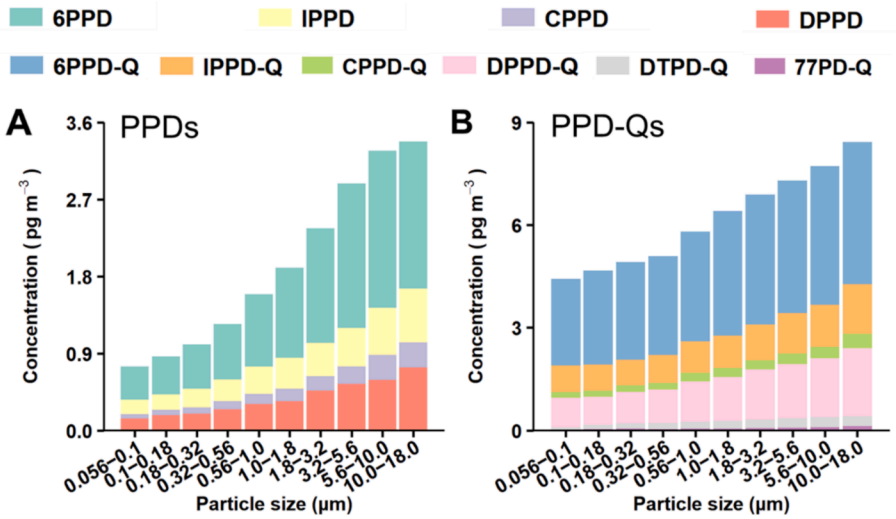

Fig. 2. Composition profiles of atmospheric PPDs (**A**) and PPD-Qs (**B**) in different sized particles (with size range of 0.056 – 18 μm) in Hefei. Shown are median concentrations.

that the observed PPD-Qs are possibly formed from the transformation of PPDs.

3.2. Size dependence of atmospheric PPDs and PPD-Qs

To provide insights into the particle size distribution of PPDs and PPD-Qs, the size-fractioned particle samples collected in Hefei (size range 0.056 – 18 μm) were analyzed. As shown in Fig. 2A and B, both PPDs and PPD-Qs exhibited clear size-dependent trends: their concentrations increased with increasing particle size. For example, the median concentrations of 6PPD-Q and IPPD-Q in the particles with size range of 10 – 18 μm (4.2 and 1.5 pg m^{-3}, respectively) were 31 % and 88 % higher than those in smaller particles with size range of 0.056 – 0.1 μm (3.2 and 0.8 pg m^{-3}, respectively), respectively. The observed size-dependent trend of PPD-Qs is in agreement with a previous measurement report of indoor airborne 6PPD-Q in waste recycling plants (Zhang et al., 2022a). The size distribution of PPDs and PPD-Qs may be rationalized through the analysis of the physicochemical properties of tire wear particles (TWPs). Previous laboratory measurements of airborne TWPs formed during driving demonstrated that coarse particles accounted for up to 70 % of the mass of TWPs (Kim and Lee, 2018; Kupiainen et al., 2005). Under such a scenario, the TWP-containing PPDs and their transformation products PPD-Qs will mainly reside in coarse particles, consistent with the measurement results in Fig. 2A and B.

For particles with a given size, the measured mean concentration of 6PPD-Q in Hefei air (e.g., 2.8 pg m^{-3} for particles with size range of 5.6 – 10 μm) was much lower than the previously reported concentration in waste recycling plants (e.g., 20.5 pg m^{-3} for particles with size range of 5.8 – 9 μm) (Zhang et al., 2022a). The lower 6PPD-Q concentration in Hefei air can be expected given that the emission intensity of airborne organic contaminants are generally higher in waste recycling plants than in outdoor environments (Hu et al., 2019; Yue et al., 2022; Zhang et al., 2019).

In addition, the size distribution of PPD-Qs is distinct from other emerging contaminants such as organophosphate esters (OPEs) (Li et al., 2021). It was found that atmospheric OPEs [e.g., tricresyl phosphate, and tris(2-butoxyethyl) phosphate] were mainly distributed in particles with aerodynamic diameter below 1.8 μm (i.e., in fine particles) (Li et al., 2021). The size distribution difference between PPD-Qs and OPEs can be attributed to their different emission sources (see further discussion in SI Text S4). As noted above, tire abrasion has been suggested as a major contributor to atmospheric PPDs and PPD-Qs (Johannessen et al., 2022a; Tian et al., 2021). In the case of OPEs, their sources are more complex, which include vaporization and mechanical abrasion of OPE-containing commercial products (e.g., building materials, furniture, and electronic devices) used in both indoor and outdoor environments (Cao et al., 2019a; Cao et al., 2022b). Given this, atmospheric PPD-Qs can be potentially used as marker compounds to evaluate the air pollution exposure related to vehicle tires in future studies.

3.3. Impact of seasonal variation and particle size on the formation of PPD-Qs

To elucidate the atmospheric behaviors of PPD-Qs, below we analysis the impact of seasonal variation and particle size on PPDs-to-PPD-Qs transformation chemistry.

3.3.1. Seasonal variation

The ratio of product PPD-Q to parent PPD concentration ($R_{PPD\text{-}Q/PPD}$) in atmospheric particles represents the extent of atmospheric oxidation. As shown in Fig. 3A, for the investigated four PPD-Q – PPD pairs (6PPD-Q – 6PPD, IPPD-Q – IPPD, CPPD-Q – CPPD, and DPPD-Q – DPPD), their $R_{PPD\text{-}Q/PPD}$ for PM_{18} in Hefei air are up to 54.3 % higher in summer than in winter. The seasonality for $R_{PPD\text{-}Q/PPD}$ may be caused by two reasons. First, the atmospheric oxidation reaction rate of PPDs can be enhanced with increasing temperature (the mean temperature in Hefei during summer and winter is 27.1 and 11.3 ℃, respectively) (Weyrauch et al., 2023; Zhao et al., 2024). Second, the measured mean ozone mixing ratio and mean solar radiation intensity in summer (45.2 ppb and 242 W m^{-2}, respectively) are significantly higher than in winter (mean ozone mixing ratio 28.4 ppb; mean solar radiation intensity 109 W m^{-2}). The higher levels of atmospheric ozone as well as strong light intensity in summer (relative to winter) will also facilitate the transformation reactions of PPDs, as demonstrated by previous experimental studies on 6PPD reactions with ozone and with sunlight (Fohet et al., 2023; Weyrauch et al., 2023; Zhao et al., 2024). These factors (temperature, ozone level, and light intensity) can enhance the formation of PPD-Qs during summer.

3.3.2. Impact of particle size

It is interesting to note that fine particles possess higher $R_{PPD\text{-}Q/PPD}$ compared to coarse particles. For example, the mean value of $R_{6PPD\text{-}Q/6PPD}$ for particles with size range of 0.056 – 0.1 μm is 3 times higher than that with size range of 10 – 18 μm (Fig. 3B). Similar $R_{PPD\text{-}Q/PPD}$ trends have also been observed for other PPD-Q – PPD pairs (IPPD-Q – IPPD, CPPD-Q – CPPD, and DPPD-Q – DPPD), as shown in Fig. 3B. One potential mechanism explaining such a difference in the oxidation levels of PPDs between different sized particles is that their heterogeneous reactivity is strongly dependent on the surface area-to-volume ratio (SA/V) of particles. A previous experimental study on heterogeneous OH oxidation kinetics of particle-bound squalane showed that the squalane reactivity in small particles (SA/V 0.42 nm^{-1}) was 37 % higher than that in large particles (SA/V 0.26 nm^{-1}) (Lim et al., 2017). This suggests that

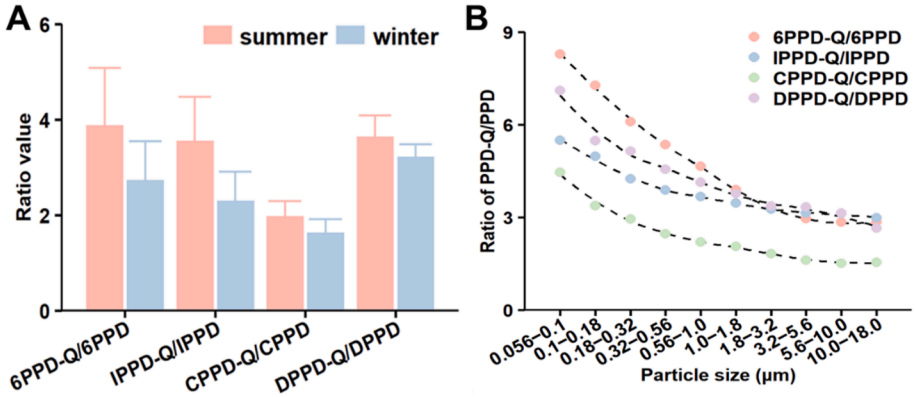

Fig. 3. (**A**) Comparison of the ratio of PM_{18} -bound PPD-Q to PPD concentrations ($R_{PPD\text{-}Q/PPD}$) during different seasons (summer and winter) in Hefei. (**B**) Comparison of $R_{PPD\text{-}Q/PPD}$ (mean value) between different sized particles (0.056 – 18 μm) in Hefei. The measurement results in B are based on summer data, while the measurement results in winter are shown in Fig. S8. The dashed lines are guides for the eye only.

organic particles with a higher SA/V will have a higher heterogeneous reaction rate. Following this logic, the transformation rate of particle-bound PPDs will likely increase with decreasing particle size (i.e., increasing SA/V; see Fig. S3), leading to a higher $R_{PPD\text{-}Q/PPD}$ for small-sized particles.

In addition, another possible reason explaining the observed $R_{PPD\text{-}Q/PPD}$ difference in Fig. 3B is that ozone is constrained within a reacto-diffusive depth (d) in atmospheric particles during gas-particle reactions. The reacto-diffusive depth represents the depth to which gaseous ozone diffuses in particles while reacting with particle-bound organics (Alpert et al., 2019; Berkemeier et al., 2016). That means below this depth in particles, ozone is unable to penetrate. At the present time, the d_{ozone} in atmospheric particles is unavailable. However, previous studies demonstrated that d_{ozone} in several organics with diverse structure were in the range of 0.9 − 70 nm (see Table S4) (Katrib et al., 2004; Lee and Wilson, 2016; Steimer et al., 2014; Wylie and Abbatt, 2020; Zhou et al., 2019). Here, by assuming that the d_{ozone} in atmospheric particles is 30 nm (i.e., within the previously reported range), we estimate the ratio of ozone-reacting volume to the total particle volume (R_{react}) for different sized-particles. Taking spherical particles with radius of 100 and 1,000 nm for example, the R_{react} of 100 nm particles (R_{react} = 0.66) is 7.3 times higher than that of 1,000 nm particles (R_{react} = 0.09; see Fig. S3). Note that a higher R_{react} reflects a higher possibility for particle-bound PPDs to interact with ozone to form PPD-Qs. Consequently, small-sized particles (i.e., having a higher R_{react}) will likely possess a higher $R_{PPD\text{-}Q/PPD}$, consistent with the results in Fig. 3B.

3.4. Human exposure assessment

Based on the median concentrations of PM_{18}-bound PPDs and PPD-Qs in Hefei air, the EDI of these emerging contaminants through ambient air inhalation for different subpopulation groups (children and adults) were assessed. The EDI of total PPDs and PPD-Qs for children were calculated to be 5.4 and 17.1 pg kg bw^{-1} d^{-1}, respectively (for adults: 3.1 and 9.5 pg kg bw^{-1} d^{-1}, respectively). These calculated EDI levels for atmospheric PPD-Qs are significantly higher than those in Hong Kong (0.18 − 0.27 pg kg bw^{-1} d^{-1}) (Cao et al., 2022a), but are lower than those in Guangzhou and Taiyuan (161 − 734 pg kg bw^{-1} d^{-1}) (Wang et al., 2022b). In comparison to the EDIs through inhalation of other emerging contaminants such as OPEs, liquid crystal monomers (LCMs), and per- and polyfluoroalkyl substances (PFAS), the reported EDIs here are much lower than those of OPEs assessed in Guangzhou (48,000 − 135,000 pg kg bw^{-1} d^{-1}) (Hu et al., 2019), and are comparable to those of LCMs (11.8 − 26 pg kg bw^{-1} d^{-1}) and PFAS (9 − 17.3 pg kg bw^{-1} d^{-1}) assessed in Guangdong province, China (Liu et al., 2023; Yao et al., 2023). In addition, these EDI levels are higher than the reported values for atmospheric benzothiazole and its derivatives (BTHs, another group of rubber-related contaminants) in Tianjing (2.3 − 4.1 pg kg bw^{-1} d^{-1}) (Zhang et al., 2018). The potential health risk induced by long-term human exposure to airborne PPD-Qs need to be considered.

The contribution of particles with different sizes to the internal exposure of PPD-Qs (represented by EBCs) was analyzed using the screening-level human exposure model, with results shown in Fig. 4. The particle size attribution of EBCs of PPD-Qs exhibits a bimodal distribution pattern (with peaked contributions at particle size of 0.056 − 0.1 μm and 1.0 − 1.8 μm), which is distinct from the size distribution of atmospheric PPD-Qs (PPD-Q concentration increases with increasing particle size; see Fig. S4). As shown in Fig. S5, assuming that the particle-bound PPD-Qs deposited onto the lung possess the same bioavailability, the particle deposition efficiency and the size distribution of PPD-Qs are the two major factors that influence the internal exposure result. Thus, the EBC data in Fig. 4 reflects the result of a combination of these factors. For example, particles with size range of 0.056 − 0.1 μm have lower PPD-Q concentrations but higher deposition efficiency in the pulmonary alveoli region (compared to particles with size range of 10 − 18 μm),

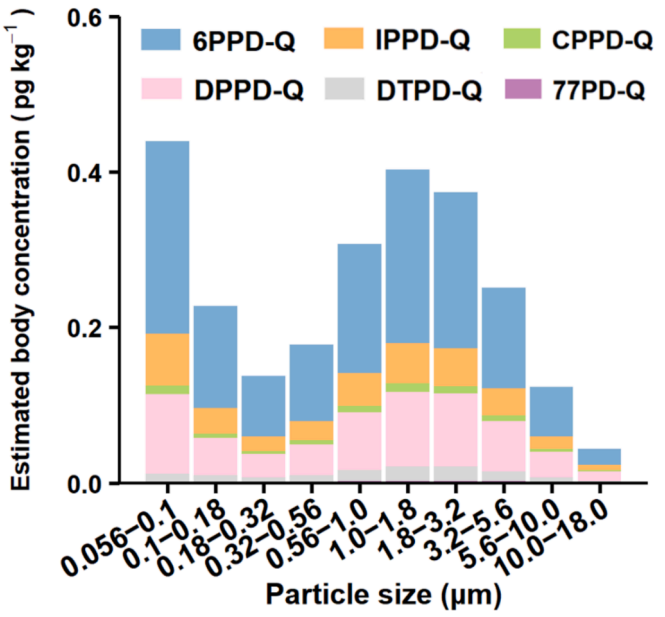

Fig. 4. The estimated body concentration for PPD-Qs bonded to different sized particles. The concentrations are estimated using a screening-level human model with the consideration of atmospheric PPD-Q levels in Hefei (see SI Text S3).

leading to a higher EBC for small-sized particles.

While the EBCs can be used for ranking chemicals of interest as an indicator of their internal exposure potential, it is noteworthy that the human model used in this study is a screening level generic exposure model with a number of assumptions/simplifications. With a one-box model, the EBCs represent concentrations in blood stream of the body as a whole, but in reality the concentrations of chemicals in blood streams at different location of the body vary significantly because different organs contribute differently on accumulating, metabolizing, and eliminating the chemicals (Peyret and Krishnan, 2011). The model uncertainty not only comes from the model structure and assumptions, but also from the model input values which are mostly QSAR estimated (e.g., partition coefficient) due to the lack of experimental values. The uncertainty can be further evaluated once the measured body concentrations of a population become available, which also allow the human model to be refined and evaluated to further reduce the uncertainty of EBCs. Regardless, the modelling results indicate that the internal exposure of particle-bound PPD-Qs can be different from their external exposure and is particle size dependent. As such, the particle size effect should be considered critical when assessing the exposure risk of atmospheric PPD-Qs.

3.5. Cellular ROS formation

As a recently discovered emerging contaminant, in addition to the atmospheric behaviors of PPD-Qs, we also need to consider their potential health impacts. ROS play an essential role in the health effects of particle-bound contaminants (Bates et al., 2019). Oxidative stress occurs when ROS level is in excess of the cellular antioxidant capacity, leading to a redox state change in cells that, in turn, can induce inflammation in the respiratory tract and cardiovascular systems (Sies et al., 2017). Thus, the capacity of contaminants to generate ROS (i.e., oxidative potential) has been suggested as a promising metric to evaluate their health effects (Bates et al., 2019; Daellenbach et al., 2020).

As shown in Fig. 5, exposure to PPD-Qs (6PPD-Q, IPPD-Q, CPPD-Q, and 77PPD-Q; 1 μM dosage) resulted in a significant increase in ROS levels in hCMEC-D3 cells. Specifically, the fluorescence intensity of DCF (an indicator for ROS level) in PPD-Q experiments was up to 69 % higher

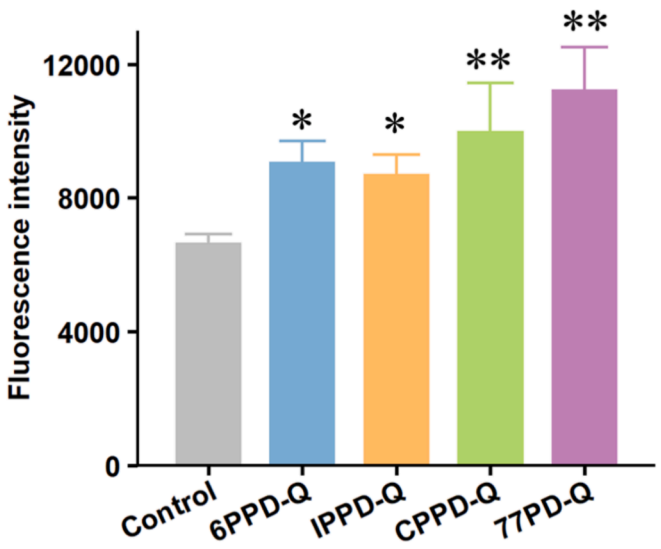

Fig. 5. Cellular ROS measurement results from the exposure of hCMEC-D3 cells to PPD-Qs (at 1 μM dosage; n = 5). The fluorescence intensity of DCF is an indicator for ROS level. The experimental results for PPD-Qs at different dosage (0.01 – 1 μM; n = 5) are shown in Fig. S6. The signal in control group is likely caused by the impurities in solution (Mohamud Yusuf et al., 2024). Mann – Whitney *U* test: * $p < 0.05$, ** $p < 0.01$.

than that in control experiments. A positive relationship between the PPD-Q dosage and cellular ROS levels was also observed in the dose-dependent experiments (0.1 – 1 μM PPD-Q; see Fig. S6). The underlying mechanism for PPD-Qs to produce ROS is likely related to their quinone structure. It is known that quinones possess redox-cycling capability and can catalyze electron transfer from cellular antioxidants (e.g., glutathione) to molecular oxygen, which will result in the formation of ROS such as hydroxyl radical and hydrogen peroxide (Charrier and Anastasio, 2012; Sies et al., 2017). The ROS measurement results in Fig. 5 are consistent with a previous acellular experiment on PPD-Qs which found that PPD-Qs had strong capacity to consume dithiothreitol (DTT; i.e., having high DTT activity) (Wang et al., 2022a). Together, both the results from cellular and acellular experiments indicate that PPD-Qs have the potential to induce oxidative stress in cells and may cause negative health impact.

In addition, a recent study found that the oxidative potential of PPD-Qs contributed to up to 5.2 % of the oxidative potential of atmospheric particles in megacities in China (Wang et al., 2022a). The results confirm that the health risk induced by atmospheric PPD-Qs is non-negligible. Recent animal studies also demonstrate that 6PPD-Q can induce a wide range of negative effects, including neurotoxicity, developmental toxicity, intestinal toxicity, reproductive toxicity, and lipid accumulation (Brinkmann et al., 2022; Fang et al., 2023; He et al., 2024; Hua and Wang, 2023a, b). The toxicity studies of other PPD-Qs (e.g., IPPD-Q and CPPD-Q) are relatively less compared to those of 6PPD-Q (Yang et al., 2024; Zhang et al., 2024). This calls for more research on the toxicity of IPPD-Q and CPPD-Q, to gain a more comprehensive understanding of the health effect of these emerging contaminants.

4. Conclusions

The present work provides new insights into the size dependence and human exposure of atmospheric PPD-Qs, which have important implications for future studies of these emerging contaminants, as discussed below.

First, it is essential to obtain accurate concentrations of PPD-Qs in air. Only by doing so can we accurately evaluate the exposure risk of airborne PPD-Qs. As mentioned above, previous studies on airborne PPD-Q mainly focused on the measurements in fine particles (Tian et al., 2024; Wang et al., 2022b; Zhang et al., 2022b). Our results demonstrate that a considerable portion of atmospheric PPD-Qs (48 % in mass) reside in coarse particles (see Fig. S7). This indicates that the previously reported atmospheric PPD-Q concentrations as well as the corresponding human exposure dosages are likely to be significantly underestimated. The present work underscores the need to analyze coarse particle-bound PPD-Qs in future field measurements. Otherwise an accurate monitoring and exposure risk assessment for these contaminants cannot be achieved.

Second, in recent years, substantial attention has been paid to the chemical transformation of airborne emerging contaminants such as PPDs and OPEs (Liu et al., 2021; Tian et al., 2021). One of the key issues regarding atmospheric transformation chemistry of emerging contaminants is their reactivity. Emerging contaminants (including PPDs) can be distributed in different sized particles, however, fundamental knowledge of their reactivity is still lacking. Here, through the analysis of the concentrations of PPD-Q – PPD pairs in different sized particles, we confirm for the first time that particle size can significantly impact the atmospheric reactivity of PPDs, i.e., PPDs in small particles tend to have a higher reactivity compared to those in large particles. Given this, the likelihood is high that other emerging contaminants (e.g., OPEs) will have similar particle size effect during atmospheric transformation. Therefore, this size effect needs to be considered when assessing the atmospheric persistence of emerging contaminants.

Third, from a health perspective, our results highlight the key role of particle size in evaluating the human exposure of PPD-Qs. The exposure assessment of PPD-Qs indicates that the internal exposures to PPD-Qs are strongly related to the size of atmospheric particles (Fig. 4). Therefore, when evaluating the health effect of airborne emerging contaminants (including PPD-Qs), the impact of particle size on human exposure should be taken into account (which has rarely been considered in previous studies) (Liu et al., 2023; Liu et al., 2020; Wang et al., 2022b; Zhang et al., 2022b). This will contribute to a more complete understanding of the health risks associated with atmospheric PPD-Qs.

CRediT authorship contribution statement

Kaihui Xia: Writing – review & editing, Writing – original draft, Methodology, Data curation, Conceptualization. **Meng Qin:** Writing – original draft, Methodology, Investigation, Data curation. **Mingming Han:** Methodology, Investigation, Data curation. **Xianming Zhang:** Methodology, Investigation, Data curation. **Xiaoguo Wu:** Methodology, Investigation. **Mingyuan Liu:** Resources, Investigation. **Shang Liu:** Resources, Investigation. **Xinkai Wang:** Methodology, Investigation. **Wei Liu:** Investigation. **Zhouqing Xie:** Resources, Investigation. **Renmin Yuan:** Data curation. **Qifan Liu:** Writing – review & editing, Writing – original draft, Supervision, Resources, Methodology, Investigation, Funding acquisition, Conceptualization.

Declaration of competing interest

The authors declare that they have no known competing financial interests or personal relationships that could have appeared to influence the work reported in this paper.

Acknowledgments

We thank Sheng-Shi Mei, Cheng-Cheng Liu, Hanyang Liu, Yuan Xue, and Jingyi Chen for the technical support with sample analysis. This work is supported by the National Natural Science Foundation of China (NSFC; 42275101), National Key Research and Development Program of China (2023YFC3710400), Beijing National Laboratory for Molecular Sciences (BNLMS2023012), and Scientific Research Foundation of Anhui Province Education Department (2023AH053401). This work was partially carried out at the Instruments Center for Physical Science, University of Science and Technology of China.

Appendix A. Supplementary data

Supplementary data to this article can be found online at https://doi.org/10.1016/j.envint.2025.109329.

Appendix C. Supplementary data

Supplementary data to this article can be found online at https://doi.org/10.1016/j.envint.2025.109329.

Data availability

Data will be made available on request.

References

Alpert, P.A., Arroyo, P.C., Dou, J., Krieger, U.K., Steimer, S.S., Foerster, J.-D., Ditas, F., Poehlker, C., Rossignol, S., Passananti, M., Perrier, S., George, C., Shiraiwa, M., Berkemeier, T., Watts, B., Ammann, M., 2019. Visualizing reaction and diffusion in xanthan gum aerosol particles exposed to ozone. Phys. Chem. Chem. Phys. 21, 20613–20627.

Arnot, J.A., Brown, T.N., Wania, F., 2014. Estimating screening-level organic chemical half-lives in humans. Environ. Sci. Technol. 48, 723–730.

Bates, J.T., Fang, T., Verma, V., Zeng, L., Weber, R.J., Tolbert, P.E., Abrams, J.Y., Sarnat, S.E., Klein, M., Mulholland, J.A., Russell, A.G., 2019. Review of acellular assays of ambient particulate matter oxidative potential: Methods and relationships with composition, sources, and health effects. Environ. Sci. Technol. 53, 4003–4019.

Bennett, D.H., Margni, M.D., McKone, T.E., Jolliet, O., 2002. Intake fraction for multimedia pollutants: A tool for life cycle analysis and comparative risk assessment. Risk Anal. 22, 905–918.

Berkemeier, T., Steimer, S.S., Krieger, U.K., Peter, T., Poeschl, U., Ammann, M., Shiraiwa, M., 2016. Ozone uptake on glassy, semi-solid and liquid organic matter and the role of reactive oxygen intermediates in atmospheric aerosol chemistry. Phys. Chem. Chem. Phys. 18, 12662–12674.

Brinkmann, M., Montgomery, D., Selinger, S., Miller, J.G.P., Stock, E., Alcaraz, A.J., Challis, J.K., Weber, L., Janz, D., Hecker, M., Wiseman, S., 2022. Acute toxicity of the tire rubber-derived chemical 6PPD-quinone to four fishes of commercial, cultural, and ecological importance. Environ. Sci. Technol. Lett. 9, 333–338.

Brown, T.N., 2014. Predicting hexadecane-air equilibrium partition coefficients (L) using a group contribution approach constructed from high quality data. Sar and Qsar Environ. Res. 25, 51–71.

Brown, T.N., Arnot, J.A., Wania, F., 2012. Iterative fragment selection: A group contribution approach to predicting fish biotransformation half-lives. Environ. Sci. Technol. 46, 8253–8260.

Cao, D., Lv, K., Gao, W., Fu, J., Wu, J., Fu, J., Wang, Y., Jiang, G., 2019a. Presence and human exposure assessment of organophosphate flame retardants (OPEs) in indoor dust and air in Beijing. China. Ecotox. Environ. Safe. 169, 383–391.

Cao, G., Wang, W., Zhang, J., Wu, P., Zhao, X., Yang, Z., Hu, D., Cai, Z., 2022a. New evidence of rubber-derived quinones in water, air, and soil. Environ. Sci. Technol. 56, 4142–4150.

Cao, G., Wang, W., Zhang, J., Wu, P., Qiao, H., Li, H., Huang, G., Yang, Z., Cai, Z., 2023. Occurrence and fate of substituted p-phenylenediamine-derived quinones in Hong Kong wastewater treatment plants. Environ. Sci. Technol. 57, 15635–15643.

Cao, Z., Zhao, L., Zhang, Y., Ren, M., Zhang, Y., Liu, X., Jie, J., Wang, Z., Li, C., Shen, M., Bu, Q., 2019b. Influence of air pollution on inhalation and dermal exposure of human to organophosphate flame retardants: A case study during a prolonged haze episode. Environ. Sci. Technol. 53, 3880–3887.

Cao, Z., Xu, X., Zhao, Y., Du, R., Fan, Y., Wei, P., Ma, K., Zhu, Y., Huang, X., Hu, F., Hu, P., Liu, X., 2022b. Gas-particle partition and size-segregated distribution of flame retardants in indoor and outdoor air: Reevaluation on the role of fine particles in human exposure. Chemosphere 292, 133414.

Charrier, J.G., Anastasio, C., 2012. On dithiothreitol (DTT) as a measure of oxidative potential for ambient particles: Evidence for the importance of soluble transition metals. Atmos. Chem. Phys. 12, 9321–9333.

Chowdhury, P.H., He, Q., Carmieli, R., Li, C., Rudich, Y., Pardo, M., 2019. Connecting the oxidative potential of secondary organic aerosols with reactive oxygen species in exposed lung cells. Environ. Sci. Technol. 53, 13949–13958.

Daellenbach, K.R., Uzu, G., Jiang, J.H., Cassagnes, L.E., Leni, Z., Vlachou, A., Stefenelli, G., Canonaco, F., Weber, S., Segers, A., Kuenen, J.J.P., Schaap, M., Favez, O., Albinet, A., Aksoyoglu, S., Dommen, J., Baltensperger, U., Geiser, M., El Haddad, I., Jaffrezo, J.L., Prévôt, A.S.H., 2020. Sources of particulate-matter air pollution and its oxidative potential in Europe. Nature 587, 414–419.

Du, B., Liang, B., Li, Y., Shen, M., Liu, L.-Y., Zeng, L., 2022. First report on the occurrence of n-(1,3-dimethylbutyl)-n`-phenyl-p-phenylenediamine (6PPD) and 6PPD-Quinone as pervasive pollutants in human urine from South China. Environ. Sci. Technol. Lett. 9, 1056–1062.

Fang, L., Fang, C., Di, S., Yu, Y., Wang, C., Wang, X., Jin, Y., 2023. Oral exposure to tire rubber-derived contaminant 6PPD and 6PPD-quinone induce hepatotoxicity in mice. Sci. Total Environ. 869, 161836.

Fohet, L., Andanson, J.-M., Charbouillot, T., Malosse, L., Leremboure, M., Delor-Jestin, F., Verney, V., 2023. Time-concentration profiles of tire particle additives and transformation products under natural and artificial aging. Sci. Total Environ. 859, 160150.

Grange, S.K., Uzu, G., Weber, S., Jaffrezo, J.L., Hueglin, C., 2022. Linking Switzerland's PM_{10} and $PM_{2.5}$ oxidative potential (OP) with emission sources. Atmos. Chem. Phys. 22, 7029–7050.

He, W., Chao, J., Gu, A., Wang, D., 2024. Evaluation of 6-PPD quinone toxicity on lung of male BALB/c mice by quantitative proteomics. Sci. Total Environ. 922, 171220.

Hiki, K., Asahina, K., Kato, K., Yamagishi, T., Omagari, R., Iwasaki, Y., Watanabe, H., Yamamoto, H., 2021. Acute toxicity of a tire rubber-derived chemical, 6PPD quinone, to freshwater fish and crustacean species. Environ. Sci. Technol. Lett. 8, 779–784.

Hiki, K., Yamamoto, H., 2022. Concentration and leachability of N-(1,3-dimethylbutyl)-N'-phenyl-p-phenylenediamine (6PPD) and its quinone transformation product (6PPD-Q) in road dust collected in Tokyo. Japan. Environ. Pollut. 302, 119082.

Hu, Y.-J., Bao, L.-J., Huang, C.-L., Li, S.-M., Zeng, E.Y., 2019. A comprehensive risk assessment of human inhalation exposure to atmospheric halogenated flame retardants and organophosphate esters in an urban zone. Environ. Pollut. 252, 1902–1909.

Hua, X., Wang, D., 2023a. Exposure to 6-PPD quinone at environmentally relevant concentrations inhibits both lifespan and healthspan in C. elegans. Environ. Sci. Technol. 57, 19295–19303.

Hua, X., Wang, D., 2023b. Tire-rubber related pollutant 6-PPD quinone: A review of its transformation, environmental distribution, bioavailability, and toxicity. J. Hazard. Mater. 459, 132265.

Huang, W., Shi, Y., Huang, J., Deng, C., Tang, S., Liu, X., Chen, D., 2021. Occurrence of substituted p-phenylenediamine antioxidants in dusts. Environ. Sci. Technol. Lett. 8, 381–385.

Huntink, N.M., Datta, R.N., Noordermeer, J.W.M., 2004. Addressing durability of rubber compounds. Rubber Chem. Technol. 77, 476–511.

Jiang, N., Li, M., Wang, Z., Hao, X., Guo, Z., Guo, J., Zhang, R., Zhang, H., Chen, J., Geng, N., 2024. p-Phenylenediamines (PPDs) and 6PPD-quinone in tunnel $PM_{2.5}$: From the perspective of characterization, emission factors, and health risks. J. Hazard. Mater. 480, 136269.

Johannessen, C., Liggio, J., Zhang, X.M., Saini, A., Harner, T., 2022a. Composition and transformation chemistry of tire-wear derived organic chemicals and implications for air pollution. Atmos. Pollut. Res. 13, 101533.

Johannessen, C., Saini, A., Zhang, X.M., Harner, T., 2022b. Air monitoring of tire-derived chemicals in global megacities using passive samplers. Environ. Pollut. 314, 120206.

Katrib, Y., Martin, S.T., Hung, H.-M., Rudich, Y., Zhang, H., Slowik, J.G., Davidovits, P., Jayne, J.T., Worsnop, D.R., 2004. Products and mechanisms of ozone reactions with oleic acid for aerosol particles having core−shell morphologies. J. Phys. Chem. A 108, 6686–6695.

Kim, G., Lee, S., 2018. Characteristics of tire wear particles generated by a tire simulator under various driving conditions. Environ. Sci. Technol. 52, 12153–12161.

Kuntz, V., Zahn, D., Reemtsma, T., 2024. Quantification and occurrence of 39 tire-related chemicals in urban and rural aerosol from Saxony. Germany. Environ. Int. 194, 109189.

Kupiainen, K.J., Tervahattu, H., Räisänen, M., Mäkelä, T., Aurela, M., Hillamo, R., 2005. Size and composition of airborne particles from pavement wear, tires, and traction sanding. Environ. Sci. Technol. 39, 699–706.

Lee, L., Wilson, K., 2016. The reactive–diffusive length of OH and ozone in model organic aerosols. J. Phys. Chem. A 120, 6800–6812.

Li, Q.L., Guo, M.R., Song, H., Cui, J.L., Zhan, M.D., Zou, Y., Li, J., Zhang, G., 2021. Size distribution and inhalation exposure of airborne particle-bound polybrominated diphenyl ethers, new brominated flame retardants, organophosphate esters, and chlorinated paraffins at urban open consumption place. Sci. Total Environ. 794, 148695.

Liang, B., Li, J., Du, B., Pan, Z., Liu, L.-Y., Zeng, L., 2022. E-waste recycling emits large quantities of emerging aromatic amines and organophosphites: a poorly recognized source for another two classes of synthetic antioxidants. Environ. Sci. Technol. Lett. 9, 625–631.

Lim, C.Y., Browne, E.C., Sugrue, R.A., Kroll, J.H., 2017. Rapid heterogeneous oxidation of organic coatings on submicron aerosols. Geophys. Res. Lett. 44, 2949–2957.

Liu, X., Chen, D., Yu, Y., Zeng, X., Li, L., Xie, Q., Yang, M., Wu, Q., Dong, G., 2020. Novel organophosphate esters in airborne particulate matters: Occurrences, precursors, and selected transformation products. Environ. Sci. Technol. 54, 13771–13777.

Liu, L.-S., Guo, Y.-T., Wu, Q.-Z., Zeeshan, M., Qin, S.-J., Zeng, H.-X., Lin, L.-Z., Chou, W.-C., Yu, Y.-J., Dong, G.-H., Zeng, X.-W., 2023. Per- and polyfluoroalkyl substances in ambient fine particulate matter in the Pearl River Delta, China: Levels, distribution and health implications. Environ. Pollut. 334, 122138.

Liu, R., Li, Y., Lin, Y., Ruan, T., Jiang, G., 2019. Emerging aromatic secondary amine contaminants and related derivatives in various dust matrices in China. Ecotox. Environ. Safe. 170, 657–663.

Liu, Q., Li, L., Zhang, X., Saini, A., Li, W., Hung, H., Hao, C., Li, K., Lee, P., Wentzell, J.J. B., Huo, C., Li, S.M., Harner, T., Liggio, J., 2021. Uncovering global-scale risks from commercial chemicals in air. Nature 600, 456–461.

Maceira, A., Borrull, F., Maria Marce, R., 2019. Occurrence of plastic additives in outdoor air particulate matters from two industrial parks of Tarragona, Spain: Human inhalation intake risk assessment. J. Hazard. Mater. 373, 649–659.

Mao, T., Liu, W., Deng, J., Chen, C., Jia, T., Li, H., Yin, F., 2024. p-Phenylenediamines and p-phenylenediamine quinone derivatives in rubber consumer products and typical urban dust: Sources, transformation profiles, and health risks. Environ. Int. 192, 109042.

Maurer, L., Carmona, E., Machate, O., Schulze, T., Krauss, M., Brack, W., 2023. Contamination pattern and risk assessment of polar compounds in snow melt: an integrative proxy of road runoffs. Environ. Sci. Technol. 57, 4143–4152.

McNeill, V.F., Yatavelli, R.L.N., Thornton, J.A., Stipe, C.B., Landgrebe, O., 2008. Heterogeneous OH oxidation of palmitic acid in single component and internally mixed aerosol particles: vaporization and the role of particle phase. Atmos. Chem. Phys. 8, 5465–5476.

Mohamud Yusuf, A., Borbor, M., Hussner, T., Weghs, C., Kaltwasser, B., Pillath-Eilers, M., Walkenfort, B., Kolesnick, R., Gulbins, E., Hermann, D.M., Brockmeier, U., 2024. Acid sphingomyelinase inhibition induces cerebral angiogenesis post-ischemia/reperfusion in an oxidative stress-dependent way and promotes endothelial survival by regulating mitochondrial metabolism. Cell Death Dis. 15, 650.

Peyret, T., Krishnan, K., 2011. QSARs for PBPK modelling of environmental contaminants. Sar and Qsar Environ. Res. 22, 129–169.

Rossomme, E., Hart-Cooper, W.M., Orts, W.J., McMahan, C.M., Head-Gordon, M., 2023. Computational studies of rubber ozonation explain the effectiveness of 6PPD as an antidegradant and the mechanism of its quinone formation. Environ. Sci. Technol. 57, 5216–5230.

Seiwert, B., Nihemaiti, M., Troussier, M., Weyrauch, S., Reemtsma, T., 2022. Abiotic oxidative transformation of 6-PPD and 6-PPD quinone from tires and occurrence of their products in snow from urban roads and in municipal wastewater. Water Res. 212, 118122.

Sies, H., Berndt, C., Jones, D.P., 2017. Oxidative Stress. Annu. Rev. Biochem. 86, 715–748.

Song, S., Gao, Y., Feng, S., Cheng, Z., Huang, H., Xue, J., Zhang, T., Sun, H., 2024. Widespread occurrence of two typical N, N'-substituted p-phenylenediamines and their quinones in humans: Association with oxidative stress and liver damage. J. Hazard. Mater. 468, 133835.

Steimer, S.S., Lampimaeki, M., Coz, E., Grzinic, G., Ammann, M., 2014. The influence of physical state on shikimic acid ozonolysis: a case for in situ microspectroscopy. Atmos. Chem. Phys. 14, 10761–10772.

Tian, L., Zhao, S., Zhang, R., Lv, S., Chen, D., Li, J., Jones, K.C., Sweetman, A.J., Peng, P. a., Zhang, G., 2024. Tire wear chemicals in the urban atmosphere: Significant contributions of tire wear particles to $PM_{2.5}$. Environ. Sci. Technol. 58, 16952-16961.

Tian, Z., Zhao, H., Peter, K.T., Gonzalez, M., Wetzel, J., Wu, C., Hu, X., Prat, J., Mudrock, E., Hettinger, R., Cortina, A.E., Biswas, R.G., Kock, F.V.C., Soong, R., Jenne, A., Du, B., Hou, F., He, H., Lundeen, R., Gilbreath, A., Sutton, R., Scholz, N.L., Davis, J.W., Dodd, M.C., Simpson, A., McIntyre, J.K., Kolodziej, E.P., 2021. A ubiquitous tire rubber-derived chemical induces acute mortality in coho salmon. Science 371, 185–189.

U.S. EPA (United States Environmental Protection Agency), 2011. Estimation Programs Interface (EPI) suite for microsoft windows. Washington, D.C.

U.S. EPA (United States Environmental Protection Agency), 2022. Chemical and Product Categories (CPCat) database. https://www.epa.gov/chemical-data-reporting/access-chemical-data-reporting-data#2020.

Wang, W., Cao, G., Zhang, J., Chen, Z., Dong, C., Chen, J., Cai, Z., 2022a. p-Phenylenediamine-derived quinones as new contributors to the oxidative potential of fine particulate matter. Environ. Sci. Technol. Lett. 9, 712–717.

Wang, W., Cao, G., Zhang, J., Wu, P., Chen, Y., Chen, Z., Qi, Z., Li, R., Dong, C., Cai, Z., 2022b. Beyond substituted p-phenylenediamine antioxidants: prevalence of their quinone derivatives in $PM_{2.5}$. Environ. Sci. Technol. 56, 10629–10637.

Wang, W., Cao, G.D., Zhang, J., Chang, W.X., Sang, Y.C., Cai, Z.W., 2024. Fragmentation pattern-based screening strategy combining diagnostic ion and neutral loss uncovered novel-phenylenediamine quinone contaminants in the environment. Environ. Sci. Technol. 58, 5921–5931.

Wang, F., Chen, X., Li, H., Huang, B., He, Y., Cai, Z., 2023. Determination of alkylphenols in atmospheric fine particulates in Taiyuan and Guangzhou based on atmospheric pressure gas chromatography-tandem mass spectrometry. Atmos. Environ. 309, 119928.

Weyrauch, S., Seiwert, B., Voll, M., Wagner, S., Reemtsma, T., 2023. Accelerated aging of tire and road wear particles by elevated temperature, artificial sunlight and mechanical stress — A laboratory study on particle properties, extractables and leachables. Sci. Total Environ. 904, 166679.

Wu, X., Hu, J., Yuan, Z., Wang, S., Tong, L., 2024. p-Phenylenediamines (PPDs) and PPD-quinones (PPD-Qs) in human urine and breast milk samples: urgent need for focus on PPD-Qs and the establishment of health threshold criteria. J. Hazard. Mater. 480, 136176.

Wu, Y., Venier, M., Hites, R.A., 2020. Broad exposure of the North American environment to phenolic and amino antioxidants and to ultraviolet filters. Environ. Sci. Technol. 54, 9345–9355.

Wylie, A.D.L., Abbatt, J.P.D., 2020. Heterogeneous ozonolysis of tetrahydrocannabinol: implications for thirdhand cannabis smoke. Environ. Sci. Technol. 54, 14215–14223.

Yang, Y.C., Meng, W., Zhang, Y., Meng, W.K., Li, J.H., Liu, W., Su, G.Y., 2024. Characterizing the metabolism of tire rubber-derived-phenylenediamine quinones to identify potential exposure biomarkers in humans. Environ. Sci. Technol. 58, 18098–18108.

Yao, L.-L., Wang, J.-L., Xu, R.-F., Zhu, M., Ma, Y., Tang, B., Lu, Q.-Y., Cai, F.-S., Yan, X., Zheng, J., Yu, Y.-J., 2023. Occurrence of liquid crystal monomers in indoor and outdoor air particle matters (PM_{10}): implications for human exposure indoors. Sci. Total Environ. 905, 166964.

Yue, C., Ma, S., Liu, R., Yang, Y., Li, G., Yu, Y., An, T., 2022. Pollution profiles and human health risk assessment of atmospheric organophosphorus esters in an e-waste dismantling park and its surrounding area. Sci. Total Environ. 806, 151206.

Zeng, L., Li, Y., Sun, Y., Liu, L.-Y., Shen, M., Du, B., 2023. Widespread occurrence and transport of p-phenylenediamines and their quinones in sediments across urban rivers, estuaries, coasts, and deep-sea regions. Environ. Sci. Technol. 57, 2393–2403.

Zhang, X., Arnot, J.A., Wania, F., 2014. Model for screening-level assessment of near-field human exposure to neutral organic chemicals released indoors. Environ. Sci. Technol. 48, 12312–12319.

Zhang, S., Cheng, Z., Cao, Y., He, F., Zhao, L., Baqar, M., Zhu, H., Zhang, T., Sun, H., 2024. Aromatic amine antioxidants (AAs) and p-phenylenediamines-quinones (PPD-Qs) in e-waste recycling industry park: occupational exposure and liver X receptors (LXRs) disruption potential. Environ. Int. 186, 108609.

Zhang, M., Shi, J., Meng, Y., Guo, W., Li, H., Liu, X., Zhang, Y., Ge, H., Yao, M., Hu, Q., 2019. Occupational exposure characteristics and health risk of PBDEs at different domestic e-waste recycling workshops in China. Ecotox. Environ. Safe. 174, 532–539.

Zhang, Y.-J., Xu, T.-T., Ye, D.-M., Lin, Z.-Z., Wang, F., Guo, Y., 2022a. Widespread n-(1,3-dimethylbutyl)-n'-phenyl-p-phenylenediamine quinone in size-fractioned atmospheric particles and dust of different indoor environments. Environ. Sci. Technol. Lett. 9, 420–425.

Zhang, Y., Xu, C., Zhang, W., Qi, Z., Song, Y., Zhu, L., Dong, C., Chen, J., Cai, Z., 2022b. p-Phenylenediamine antioxidants in $PM_{2.5}$: The underestimated urban air pollutants. Environ. Sci. Technol. 56, 6914–6921.

Zhang, J., Zhang, X., Wu, L., Wang, T., Zhao, J., Zhang, Y., Men, Z., Mao, H., 2018. Occurrence of benzothiazole and its derivates in tire wear, road dust, and roadside soil. Chemosphere 201, 310–317.

Zhao, H.N., Hu, X.M., Gonzalez, M., Rideout, C.A., Hobby, G.C., Fisher, M.F., McCormick, C.J., Dodd, M.C., Kim, K.E., Tian, Z.Y., Kolodziej, E.P., 2023a. Screening p-phenylenediamine antioxidants, their transformation products, and industrial chemical additives in crumb rubber and elastomeric consumer products. Environ. Sci. Technol. 57, 2779–2791.

Zhao, H.N., Thomas, S.P., Zylka, M.J., Dorrestein, P.C., Hu, W., 2023b. Urine excretion, organ distribution, and placental transfer of 6PPD and 6PPD-Quinone in mice and potential developmental toxicity through nuclear receptor pathways. Environ. Sci. Technol. 57, 13429–13438.

Zhao, F., Yao, J.Z., Liu, X.Y., Deng, M., Chen, X.J., Shi, C.Z., Yao, L., Wang, X.F., Fang, M. L., 2024. Occurrence and oxidation kinetics of antioxidant-phenylenediamines and their quinones in recycled rubber particles from artificial turf. Environ. Sci. Technol. Lett. 11, 335–341.

Zhou, Z., Zhou, S., Abbatt, J.P.D., 2019. Kinetics and condensed-phase products in multiphase ozonolysis of an unsaturated triglyceride. Environ. Sci. Technol. 53, 12467–12475.

Zhu, J., Guo, R., Jiang, S., Wu, P., Jin, H., 2024. Occurrence of p-phenylenediamine antioxidants (PPDs) and PPDs-derived quinones in indoor dust. Sci. Total Environ. 912, 169325.

Zoroufchi Benis, K., Behnami, A., Minaei, S., Brinkmann, M., McPhedran, K.N., Soltan, J., 2023. Environmental occurrence and toxicity of 6PPD Quinone, an emerging tire rubber-derived chemical: a review. Environ. Sci. Technol. Lett. 10, 815–823.